
Article:
Rigby, S.E., Tyas, A. orcid.org/0000-0001-6078-5215 and Bennett, T. (2012) Single-Degree-of-Freedom response of finite targets subjected to blast loading – The influence of clearing. Engineering Structures, 45. pp. 396-404. ISSN 0141-0296

https://doi.org/10.1016/j.engstruct.2012.06.034

Single-Degree-of-Freedom Response of Finite Targets Subjected to Blast Loading – The Influence of Clearing

S.E. Rigby[a], A. Tyas[a], T. Bennett[a,*]

[a]*Department of Civil & Structural Engineering, University of Sheffield, Mappin Street, Sheffield, S1 3JD, UK*

Abstract

When evaluating the dynamic response of a structure subjected to a high explosive detonation, it is common to simplify both the target properties and the form of the blast pressure load – a standard approach is to model the target as an equivalent Single-Degree-of-Freedom (SDOF) system with the blast load idealised as a pulse which decays linearly with time. Whilst this method is suitable for cases where the reflecting surface is large, it is well known that for smaller targets, the propagation of a rarefaction 'clearing' wave from the edges of the target may cause a premature reduction in the magnitude of the blast pressure and hence reduce the total impulse acting on the structure. In this article, a simple method for calculating clearing relief, based on an acoustic approximation of the rarefaction wave, is coupled with an SDOF model to investigate the influence of clearing on the dynamic response of elastic targets. Response spectra are developed for a range of target sizes and blast events that may be of interest to the engineer, enabling the effects of blast wave clearing to be evaluated and situations where blast wave clearing may increase the peak displacement of the target to be determined. When the natural period of the target is large compared to the duration of loading, the reduction in positive phase impulse leads to significantly lower values of peak displacement when compared to an identical system subjected to a triangular blast load. For systems where the natural period is comparable to the duration of the loading, the early onset of negative pressure (attributed to blast wave clearing) can coincide with the rebound of the target and result in greater peak displacements. It is concluded that blast wave clearing should be evaluated and its influence quantified in order to ensure that blast resistant designs are efficient and safe.

Keywords: blast loading, clearing, finite target, response spectra

1. Introduction

The potentially devastating effects of a high explosive detonation, coupled with a perceived increase in the use of such weaponry against civilian targets, has highlighted the need to analyse and design structures to resist such extreme loading events. In order to ensure that a structure can respond safely to a high explosive detonation, the loading imparted on the target, and hence the response of the system must be quantified with a sufficient level of confidence.

Numerical analysis methods are a valuable design tool, however the associated computational expense often renders such methods impractical for use in the early stages of design. It is often more desirable to undertake quick, approximate calculations to refine a scheme before more complex analyses are undertaken, however this is normally facilitated by simplifying the load model subjected to the target.

The empirical load model proposed by Kingery and Bulmash [1] – implemented into the U.S. Department of Defense Design manual UFC-3-340-02 [2] (previously TM-5-1300), automated predictive tool ConWep [3], and Blast Effects Design Spreadsheet (SBEDS) [4] – provides predictions for the blast pressure acting on an infinite target.

It is well known that a relief wave, travelling inwards from the edges of a finite target, can reduce the late time pressure acting on the loaded face. Current design guidance [2, 3, 4] provides simple corrections to account for this pressure reduction, however recent studies have questioned the validity of this approach [5, 6] and suggested improved empirical corrections for the clearing effect. In fact, as discussed in recent articles by the current authors [7, 8], a simple, yet robust approach to predicting clearing relief was developed almost 60 years ago at Sandia National Laboratory [9]. This article investigates the effect of this clearing relief on the dynamic response of finite targets.

2. Blast Loading on an Infinite Target

Following an explosive detonation, the rapid conversion of the reacting material into high temperature, high pressure gas displaces the surrounding medium (typically air) at a rapid rate, causing a shock wave to form. This shock wave travels outwards from the source of the explosion

*Tel.: +44 (0) 114 222 5765
Email address: t.bennett@shef.ac.uk (T. Bennett)

and is characterized by an abrupt increase in pressure, p_{max}, followed by an exponential decay to ambient pressure, the duration of which is called the positive phase duration, t_d. After the positive phase comes a period of 'negative' (below atmospheric) pressure caused by over expansion of the air following the shock front. The pressure-time profile for an ideal blast wave in free air is shown schematically in Figure 1, where the minimum pressure is given as p_{min} and the negative phase duration is given as t_n.

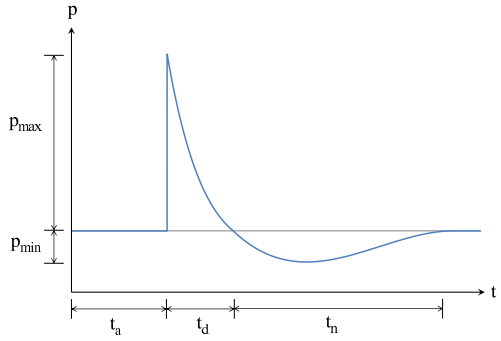

Figure 1: Idealised pressure-time profile for a blast wave in free air

If a blast wave propagates in air without encountering an obstacle, the air will be compressed to an 'incident' or 'side-on' pressure, p_{so}. When the blast wave is obstructed by a rigid target, conservation of momentum and energy at the boundary results in a significant increase of pressure, to a reflected pressure, p_r. Blast resistant design is concerned with ensuring that the structure can resist this reflected pressure and impulse.

2.1. Modelling the Positive Phase

The positive phase pressure-time history of the empirical load model [1] is approximated by the 'modified Friedlander equation' [10],

$$p(t) = p_{max}\left(1 - \frac{(t - t_a)}{t_d}\right) exp\left(\frac{-b(t - t_a)}{t_d}\right), \tag{1}$$

and the values of peak overpressure (p_{max}), arrival time (t_a), positive phase duration (t_d) and waveform parameter (the coefficient describing the rate of decay of the pressure-time curve, b) can be determined from the empirical data presented by Kingery and Bulmash [1]. This enables incident and reflected airblast parameters to be predicted for either surface bursts or free air bursts

at any scaled distance, $Z = R/W^{1/3}$, where R is the distance from the charge centre to the target, and W is the mass of explosive charge, expressed as an equivalent mass of TNT.

Using this simplified load model allows the analyst, as a first approximation, to estimate the magnitude and temporal variation of loading on a structure exposed to a blast wave, without the need to model the blast wave propagation and interaction with the structure, vastly saving on computational expense. This simple method forms the basis of design guidance such as UFC 3-340-02 [2], and software such as ConWep [3] and SBEDS [4].

2.2. Modelling the Negative Phase

It is a common approach to ignore the negative phase when using the empirical load model. Whilst this may perhaps be considered conservative, Teich et. al. [11] and Krauthammer and Altenberg [12] demonstrate that this approach can be un-conservative if the onset of negative pressures coincide with the rebound of the target.

For highly impulsive loading, neglecting the negative phase can be grossly over-conservative, particularly considering that the magnitude of negative phase impulse approaches that of the positive phase at larger scaled distances. As such, it may be important to model the negative phase accurately.

In this study, the negative phase parameters compiled by Goodman [13] are used with the cubic expression presented in the Naval Facilities Engineering Command Design Manual, *Blast Resistant Structures* [14]

$$p(t) = p_{min}\left(\frac{6.75(t - [t_a + t_d])}{t_n}\right)\left(1 - \frac{t - [t_a + t_d]}{t_n}\right)^2, \tag{2}$$

where p_{min} is the peak underpressure and t_n is the negative phase duration.

2.3. Experimental Validation

In a review of simplified blast predictive models, Bogosian et. al. [15] concluded that the ConWep method best represented the average results from a wide range of test data collected, although the full-scale experiments demonstrated a significant spread. Rickman and Murrell [5] observed that, for small scale tests, the ConWep predictions of reflected pressure agreed remarkably well with the measured pressures.

As part of the current investigation, a number of blast trials were conducted at the University of Sheffield Blast & Impact Laboratory, Buxton, UK. 0.25kg C4 hemispherical explosive charges

were detonated 4m, 6m, 8m and 10m away from a semi-infinite, rigid target[1]. The charges were detonated on a 50mm thick steel plate, placed on a level, flat concrete ground slab, enabling the detonation to be considered as a hemispherical surface burst. A Kulite HKM 7 bar pressure gauge was placed 375mm from the base of the target, with a distance of at least 4m to any free edge of the reflecting surface. Pressure was recorded using a 16-Bit Digital Oscilloscope at a sample rate of 100kHz synchronised with the detonation. Figure 2 shows experimental pressures and ConWep (positive phase) and NavFac [14] (negative phase) predictions from this study – the experimental traces show a small amount of sensor ringing at the shock front, and record the presence of the well-known 'second shock' at the beginning of the negative phase, but overall the predictions match the experimental traces remarkably well.

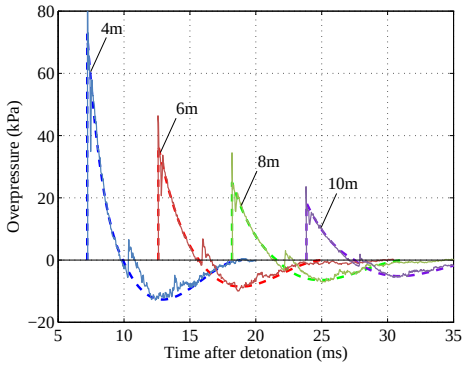

Figure 2: Experimental and predicted pressure time histories for a 0.25kg C4 (0.3kg TNT) charge detonated on a rigid surface at ranges of 4m, 6m, 8m and 10m from a semi-infinite target (Z = 6.0, 9.0, 12.0 and 14.9m/kg$^{1/3}$)

It is clear that both the positive and negative phase predictions provide a highly accurate representation of the experimentally measured pressure-time history of a high explosive detonation. The empirical load model can thus be a very useful tool for the first stages of blast-resistant design; however the method assumes that the structural geometry has no influence on the development of reflected pressures on the face of the target, i.e., that the structure is effectively infinite in size in the directions parallel to the blast wave front. When this is not the case, the propagation of a 'relief' pressure wave from the free edges of the target may influence the load applied to the structure. This process is known as 'clearing'.

[1] A 500mm thick, reinforced concrete bunker wall, 4.5m high × 4.0m long.

3. Blast Loading on a Finite Target

Clearing begins the moment a blast wave reaches the free edge of a finite reflecting surface. At this free edge, whilst the reflected shock front begins to reflect away from the surface, the incident shock front continues unimpeded past the edge of the target, causing diffraction around the free edge. This diffraction generates a low pressure rarefaction wave travelling along the loaded face, beginning at the boundaries and propagating in towards the centre of the target (see Figure 3). As it passes over a point of interest, the rarefaction wave reduces the pressure acting on the loaded face, and hence reduces the total positive phase impulse imparted to the target.

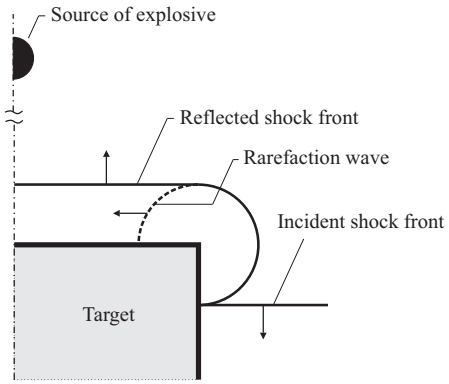

Figure 3: Diffraction of a blast wave around a finite target causing the propagation of a rarefaction clearing wave

3.1. Current Methods for Predicting Clearing

Early attempts to predict the clearing effect [2, 3] assumed a linear decay from the peak reflected overpressure to a 'stagnation pressure' over a characteristic 'clearing time'. As discussed by Rickman and Murrell [5], there are two main reasons why this approach is physically questionable:

- The approximation of a linear reflected pressure decay rather than an exponential decay.
- The assumption that the reflected pressure begins to decay *immediately* after the arrival of the shock wave. This assumption is true for the *total* load acting on the face of the target, however it cannot be valid for the pressure at a point on the target located away from a free edge, since there will be a transient time for the clearing wave to arrive. Because of this

assumption, the traditional approaches cannot be used to accurately determine the spatial variation of reflected pressures acting on the target.

The calculation of the 'clearing time' (the time at which clearing is completed and the stagnation pressure is reached) is inconsistent throughout the approximations, casting serious doubt on their validity [5]. Another problem with the traditional approach is the inability to predict the early onset of negative pressures due to clearing, which is clearly seen in the experimental results in [5] and [7]. This has been addressed by the improved methodologies of Rickmann and Murrell [5], where an empirical method for predicting clearing relief was developed from experimental data, and Rose and Smith [6], where 'clearing factors', determined from numerical analyses, are applied to the reflected impulse, based on various target geometries and scaled distances.

3.2. The Hudson Method

Tyas et al. [7, 8] present an approach to blast wave clearing predictions, first developed by Hudson [9]. The rarefaction relief wave is approximated as an acoustic pulse initiating at the edge of the target and travelling inwards along the loaded face. The Hudson method assumes the following conditions:

- The blast wave is plane and parallel to the target surface. This implies that the target dimensions are small relative to the charge stand-off.
- The depth of the target is sufficiently large so that no diffraction waves arrive from the rear of the target.
- The clearing wave propagates into stagnant air across the target face, i.e. no flow conditions exist in the direction of travel of the rarefaction wave.
- The velocity of the rarefaction wave is equal to the ambient sonic speed in air. This requires the incident pressure to be relatively low – Hudson judged that the assumption was reasonable for peak incident pressures of less than 300kPa i.e. $Z \geq 2.0\text{m/kg}^{1/3}$.

Predictions for the pressure acting at a point on the target face are given as a superposition of the 'clearing pressure' associated with the acoustic wave and the reflected pressure acting on an infinite target.

The temporal and spatial pressure distribution of the acoustic pulse, presented by Hudson [9], is shown in Figure 4. The non-dimensional clearing length is given as $\eta = x/a_0 t_d$, (the distance from a free edge, x, divided by the 'length' of the positive phase of the blast wave, where $a_0 = 340$m/s). Values of $\eta > 1$ indicate a point where the clearing wave arrives after the completion of the positive phase (hence one that will be subjected to the full reflected pressure for the entire positive phase), whereas $\eta = 0$ indicates a point on the free edge where clearing relief will begin immediately upon the arrival of the blast wave.

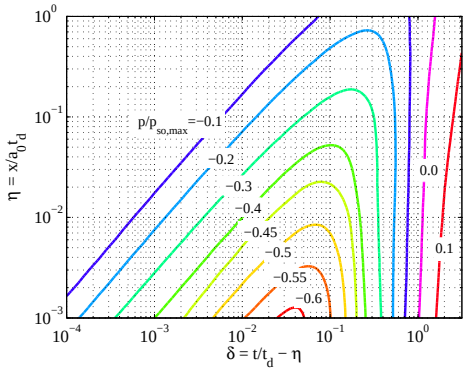

Figure 4: Contours of clearing pressure relief from acoustic theory [9]

Figure 5 shows how the Hudson method can be used to predict the pressure acting at a point on a finite target. In this example, the ConWep predictions for the blast pressure resulting from a 1kg TNT detonation at 10m are superimposed with the Hudson clearing function (Figure 4) at a distance of 0.15m from a free edge (the positive phase duration of 4.788ms gives this point a value of $\eta = 0.09$). Superposition of the ConWep predictions with the Hudson relief function at a given point, to account for blast wave clearing, has been shown to be in excellent agreement with experimental results [7].

Rose and Smith [6] and Bogosian et. al. [15] conclude that blast wave clearing is an essential consideration for $Z > 2.0\text{m/kg}^{1/3}$, and the Hudson method appears to provide a simple yet accurate means of predicting the clearing effect for simple geometries. It is the purpose of this paper to demonstrate the effect that blast wave clearing may have on the dynamic response of a structure, and to highlight the errors and conservatism that may be associated with neglecting the clearing effect.

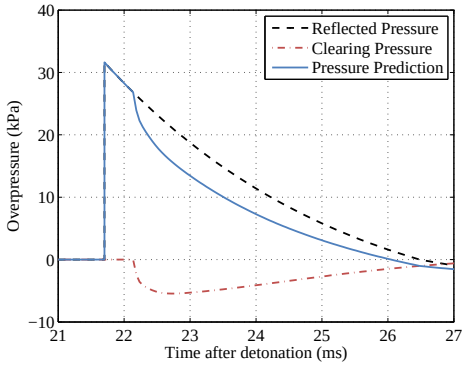

Figure 5: Prediction of pressure acting at a point 150mm ($\eta = 0.09$) from the free edge of a finite target, based on the superposition of the reflected pressure and clearing pressure (for $W = 1$kg, $R = 10$m)

4. The Influence of Clearing

4.1. Developing a Numerical Model

A Single-Degree-of-Freedom (SDOF) analysis is a common approach to determine the blast response of a structure, and requires the solution of Newton's equation of motion

$$m\ddot{z} + c\dot{z} + kz = F(t), \tag{3}$$

where m, c and k are the system mass, damping and stiffness, $\ddot{z}$, $\dot{z}$ and z are the acceleration, velocity and displacement of the system, and $F(t)$ is the externally applied load.

The motion of the entire system is described by one coordinate, i.e. the displacement at a significant point on the structure. The equivalent parameters (mass, stiffness, spring yield load and applied load) are calculated by equating the kinetic energy, internal strain energy and work done for both systems, and applying the resultant *mass factor* and *load factor* to the 'real life' parameters [16]. It is common to ignore structural damping in equivalent systems (as, typically, a low number of vibratory cycles are considered and small damping ratios have little short-term effect [12]), which gives the *equivalent* equation of motion as

$$m_e\ddot{z}(t) + k_e z(t) = F_e(t). \tag{4}$$

4.1.1. SDOF Model Under a Non-Uniform Load

The derivation of the SDOF load transformation factor for a loaded plate assumes a spatially uniform pressure – an assumption that is not valid when considering the effects of blast wave clearing. In order to ensure that the spatially varying pressure, $p(x, y, t)$, acting on the face of a target can be validly represented in an SDOF model, the *energy equivalent uniform pressure* and *spatial load factor* are derived in this section.

The energy equivalent uniform pressure acting on a target is given such that the work done at any instant is equal for both the uniform ($p_{energy,equiv}(t)$) and 'real-life' ($p(x, y, t)$) pressure, i.e.

$$\int_A p(x, y, t)\phi(x, y)\, dA = \int_A p_{energy,equiv}(t)\phi(x, y)\, dA, \tag{5}$$

where A is the panel area, and ϕ is the shape function (describing the normalised deflected shape of the target). Since the uniform pressure is independent of x and y it can be given as

$$p_{energy,equiv}(t) = \frac{\int_A p(x, y, t)\phi(x, y)\, dA}{\int_A \phi(x, y)\, dA}, \tag{6}$$

where the two-dimensional shape function can be expressed in separable variable form, $\phi(x, y) \approx \phi(x)\phi(y)$ [17] and is assumed to be constant with time.

The SDOF equivalent force is given as

$$F_e(t) = K_L F_{energy,equiv}(t) \tag{7}$$

where K_L is the load factor given by SDOF theory [16] and $F_{energy,equiv}(t)$ is the energy equivalent uniform pressure multiplied by the area of the plate. The spatial load factor, $K_{spatial}(t)$ can be defined as a time varying load factor used to transform the *total* force acting on the plate at any instant into the *energy equivalent* force, i.e. the equivalent SDOF force now becomes

$$F_e(t) = K_L K_{spatial}(t) F(t). \tag{8}$$

Equations 7 and 8 can be combined to give

$$K_{spatial}(t) F(t) = F_{energy,equiv}(t), \tag{9}$$

and from the definition of the energy equivalent force acting on the plate (equation 6 multiplied by the target area), the time varying load factor can be expressed as

$$K_{spatial}(t) = \frac{\int_A p(x,y,t)\phi(x,y)\,dA}{\int_A p(x,y,t)\,dA \int_A \phi(x,y)\,dA}. \tag{10}$$

$K_{spatial}$ is effectively a measure of the non-uniformity of the applied pressure (it can be easily seen that if the pressure is uniform, i.e. independent of x and y, $K_{spatial}(t) = 1$) and, combined with the traditional load factor, can be used to ensure that the force acting on the SDOF model is equivalent in terms of energy to the real life system for the entire duration of loading. The spatial load factor is derived using the same assumptions and conditions as the traditional load factor and ensures the analysis is consistent with the SDOF method. Although the spatial load factor is used to model the effects of blast wave clearing, it could in practice be used to transform any spatially varying load into an energy equivalent uniform load.

4.2. Numerical Example

In order to demonstrate how the consideration of clearing effects may influence the dynamic response of a target, the equivalent equation of motion (4) was solved for two undamped elastic systems subjected to the same blast load – a 1kg TNT hemispherical surface burst detonated 10m from the target. Three load cases were considered; an idealised linear decay, a full positive and negative phase acting on an infinite surface, and the pressure acting on a 2×2m target with Hudson clearing corrections.

The relevant blast load parameters are given in Table 1. The linear approximation is taken to have the same peak overpressure and impulse as the infinite load case, with a reduced loading duration. The clearing pressure was calculated by discretizing the target face into a grid of 100×100 elements and determining the Hudson clearing function at each node (Figure 4). The spatially varying pressure was then transformed into an equivalent SDOF force at each time step using equation 8. The shape functions $\phi(x)$ and $\phi(y)$ for a one-way spanning, elastic clamped beam are given in Belvins [17]. Diffraction was allowed around the top face and side faces only, i.e. the bottom edges of the plates were situated on a rigid surface.

The two targets were modelled as linear elastic, two-way spanning aluminium panels, fixed on all sides. The relevant dynamic model parameters are shown in Table 2, where the dynamic coefficients are given using the revised values from Morison [18]. The three load cases are shown in Figure 6, where the pressures have been converted into an equivalent force using the target area

Parameter		Value
Peak reflected pressure	$p_{r,max}$	31.54 kPa
Peak reflected underpressure	$p_{r,min}$	7.68 kPa
Positive phase duration	t_d	4.79 ms
Negative phase duration	t_n	14.45 ms
Positive phase impulse	i^+	59.33 kPa.ms
Negative phase impulse	i^-	62.39 kPa.ms
Linear load duration	$\bar{t}_d$	3.76 ms
Clearing positive phase duration	$t_{d,clear}$	3.39 ms
Clearing negative phase duration	$t_{n,clear}$	15.27 ms
Clearing positive phase impulse	i^+_{clear}	49.74 kPa.ms
Clearing negative phase impulse	i^-_{clear}	38.71 kPa.ms

Table 1: Loading parameters applied to the numerical model. Pressures are converted into an equivalent force using the load transformation factor, $K_L = 0.308$, and the spatial load transformation factor, $K_{spatial}$, derived in section 4.1.1

and load transformation factor, $K_L = 0.308$ (and spatial load transformation factor, $K_{spatial}(t)$ for the clearing load).

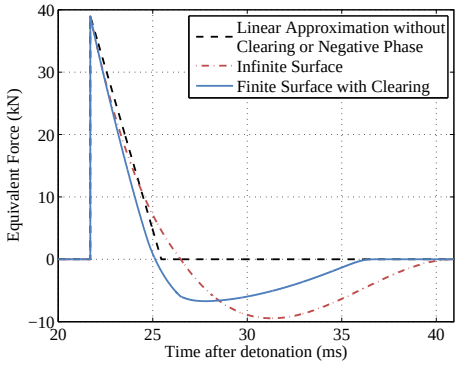

Figure 6: Three load cases applied to the numerical model

A representative parameter used in structural dynamics is the ratio of the load duration to the natural period of the structure, t_d/T. Larger values of t_d/T indicate that the target response is quick in relation to the loading duration and the loading can be considered as quasi-static,

Parameter		Plate A	Plate B
Young's modulus	E	69 GPa	69 GPa
Density	ρ	2700 kg/m^3	2700 kg/m^3
Poisson's ratio	ν	0.35	0.35
Load factor	K_L	0.308	0.308
Mass factor	K_M	0.182	0.182
Elastic stiffness coefficient	$k_e/(D/h^2)$	808.5	808.5
Height	h	2 m	2 m
Thickness	t	7 mm	27.5 mm
Equivalent stiffness	k_e	140 kN/m	8484 kN/m
Equivalent mass	m_e	13.76 kg	54.05 kg
Natural frequency	f	16.05 Hz	63.05 Hz
Natural period	T	62.31 ms	15.86 ms
Time ratio	t_d/T	0.077	0.302

Table 2: Dynamic Properties for 2 × 2m linear elastic, two-way spanning aluminium panels, fixed on all sides

whereas smaller values of t_d/T indicate that the loading is tending towards impulsive. Plate A and plate B have time ratios of 0.077 and 0.302 respectively, i.e. the two plates lie within the dynamic region of loading, and hence will be sensitive to the time-varying effects of clearing relief. The displacement-time histories of the two systems, as well as values of peak displacement, can be seen in Figure 7.

For plate A (Figure 7(a)), with the lower value of t_d/T, the decrease in positive phase impulse attributed to clearing relief results in a significantly lower value of outward displacement. The early onset of negative pressure (the shortening of the positive phase) initially serves to decrease the velocity of the plate, however when the velocity becomes negative and the plate begins to rebound, the application of negative pressure results in a greater displacement in the *inward* direction. This rebound effect, although acting to increase the value of peak displacement, is lessened by the simultaneous reduction of both negative phase duration and peak underpressure caused by blast wave clearing (Figure 6). In this case, neglecting blast wave clearing and designing for a simplified triangular load function can lead to an over-prediction of peak displacement.

For plate B (Figure 7(b)), the opposite can be said. The plate reaches its maximum positive

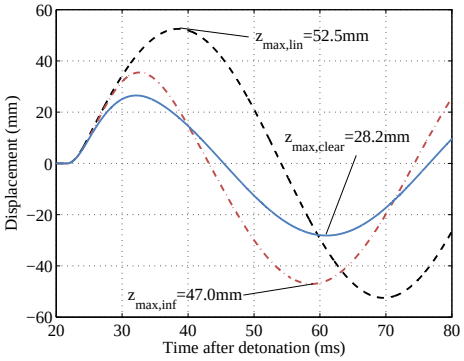

(a) Plate A

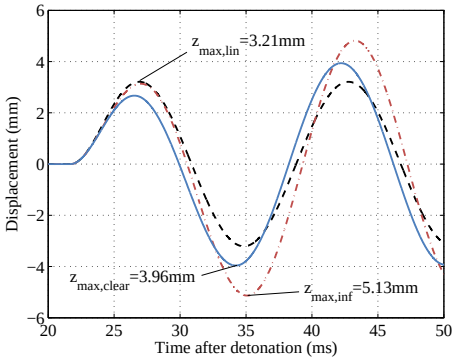

(b) Plate B

Figure 7: Displacement-time history for Plate A and Plate B under three different load cases shown in Figure 6

displacement and hence begins to rebound at roughly the same time as the beginning of the negative phase (around 26ms), resulting in a greater peak displacement than the triangular load model. The influence of clearing is to reduce both the positive and negative phase pressures and the rebound effect is less pronounced, however it still results in a greater peak displacement than the triangular load model alone. The triangular load model is thus under-conservative.

4.2.1. Verification of the Spatial Load Factor

The veracity of the spatial load factor can be highlighted using a simple example. Here, Plate B (27.5mm thick 2×2m aluminium plate) was analysed using the explicit FEM code LS-DYNA

[19]. The FE model was discretised into a grid of 100×100 elements and the pressure prediction at each node was applied as a separate time-varying force. The plate was modelled using the same material properties as those given in table 2. The SDOF model was evaluated for two load cases; the equivalent force calculated using the standard load transformation factor *and* the spatial load factor ($F_e(t) = K_L K_{spatial}(t) F(t)$) and the equivalent force calculated by using the standard load transformation factor *only* (i.e. setting the spatial load factor to unity, $F_e(t) = K_L F(t)$). Figure 8 shows the response of the SDOF model under both applied loads and the response of the FE model.

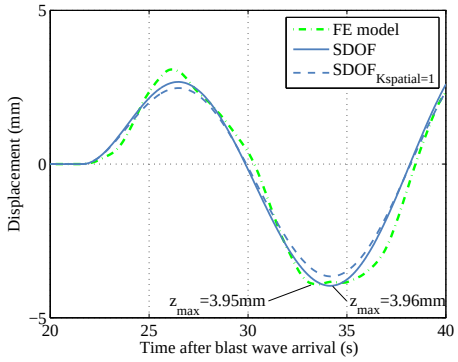

Figure 8: Verification of $K_{spatial}(t)$ by comparing Single-Degree-of-Freedom and Finite Element response

It can be seen from Figure 8 that, whilst there are some discrepancies in the early stages of deformation due to the FE model's ability to include higher modes of response, the energy equivalent load SDOF model generally exhibits excellent agreement with the FE model. In particular, there is excellent correlation in the results from the two models for the the peak displacement on the first negative half-cycle (3.95mm in the FE model compared to 3.96mm in the energy-equivalent load SDOF model). It is also apparent that an improvement in the accuracy of the model is observed when using the spatial load factor compared to the simple average pressure SDoF model.

The function $K_{spatial}(t)$ is shown in Figure 9, where the inclusion of the spatial load factor results in an increase in the applied load ($K_{spatial} > 1$ because the mid-span of the plate is more heavily loaded than the edges). There is a discontinuity in the function when the applied force goes from positive to negative as, momentarily, the denominator in equation 10 is zero.

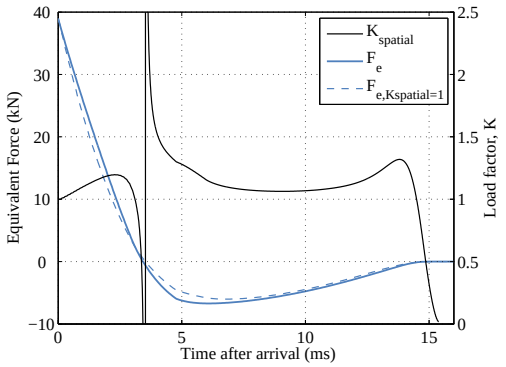

Figure 9: $K_{spatial}(t)$ and equivalent forces for a 2 × 2m elastic target subjected to a 1kg hemispherical TNT burst at 10m. F_e denotes the force calculated using the spatial load factor and $F_{e,Kspatial=1}$ denotes the force calculated from the average pressure on the plate, i.e. assuming $K_{spatial} = 1$

Equipped with a simplistic and experimentally validated means for predicting the pressure acting on a finite target [7], coupled with a valid means for implementing a non-uniform load into an SDOF model (using the time-varying spatial load factor, $K_{spatial}(t)$), a comprehensive parametric study can be undertaken.

4.3. Parametric Study

A useful parameter for determining the influence of clearing relief is the *displacement ratio*, the ratio of peak displacements of the SDOF system under the clearing and linear load respectively,

$$\text{Displacement ratio} = z_{max,clear}/z_{max,lin} \tag{11}$$

i.e. the level at which the traditional approach may under or over predict the peak elastic deformation. For plate A and plate B, the corresponding displacement ratios are 0.54 and 1.23 respectively. It is clear that consideration of clearing cannot be inherently under or over-conservative. In order to be able to determine the influence of clearing relief on a given target, the study was extended to investigate a range of target dimensions.

4.3.1. Varying Target Dimension

The clearing length to the centre of a target, η_c, is given as

$$\eta_c = h/2a_0t_d, \tag{12}$$

where h is the height of the target. For a given scaled distance, there exist many combinations of target size and charge mass that will give the same value of η_c, as is shown in Figure 10. For two targets of different physical dimensions, providing the scaled distance and *scaled target size* are the same, both will experience the same level of scaled clearing relief.

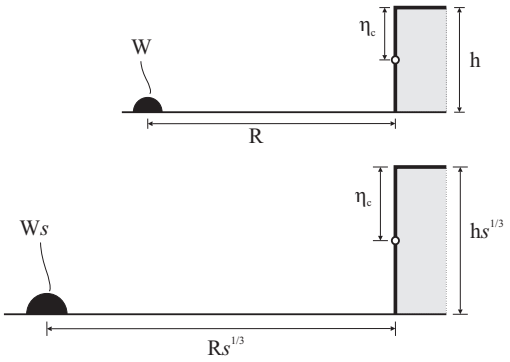

Figure 10: Scaled target dimensions giving the same value of η_c

For larger clearing lengths, the arrival time of the clearing relief wave increases and the magnitude of pressure relief decreases – hence as the target size tends to infinity, a smaller proportion of the loaded face experiences clearing relief and the blast pressure approaches the fully reflected pressure. As the target size tends to zero, the loading approaches the incident pressure [20], however for intermediate sized targets, particularly at larger scaled distances, it is known that clearing relief may 'overshoot' the incident pressure and result in the early onset of negative pressures [6, 7]. This could have a significant impact on the response of a target in the dynamic range of loading.

The influence of target size on the development of cleared pressures on the loaded face can be seen in Figure 11 – the equivalent uniform pressure (equation 6) acting on finite targets subjected to a 1kg hemispherical surface burst at a range of 10m. Given the positive phase duration, t_d = 4.79ms, values of η_c = 0.2–1.0 equate to target heights of 0.65–3.25m. Early negative pressures can be seen for all target sizes, and it can be seen that smaller targets are subjected to significantly lower positive impulse.

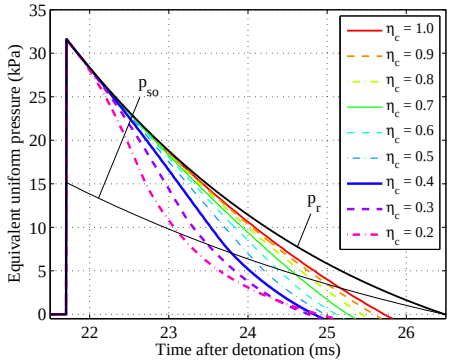

Figure 11: Equivalent uniform pressure acting on range of target sizes from a 1kg TNT detonation at 10m. η_c denotes the clearing length to the centre of the target, from equation 12

4.3.2. SDOF Response Spectra

With the numerical framework in place, it is possible to evaluate a combination of scaled distance (Z), target size (η_c) and dynamic properties (time ratio, t_d/T) to determine the influence of clearing relief on the peak elastic deformation of finite targets (i.e. the displacement ratio, $z_{max,clear}/z_{max,lin}$) over a range of target properties and blast scenarios that may be of interest to the engineer.

Figure 12 shows response spectra for linear elastic, clamped square targets subjected to blast loads at different scaled distances. The target size and dynamic properties are independent of scale and can be used to determine the effect of clearing for any blast event[2], offering a quick and simple first approximation to the influence of clearing relief.

Given a likely blast event and an estimation of the target properties, the corresponding value of displacement ratio can be easily determined from Figure 12, giving a valuable and immediate appraisal of the likely influence that clearing relief may have on the design of the structure in question. The curve for $\eta_c = \infty$ indicates an infinite sized target subjected to (non-cleared) reflected pressures. In the example outlined in section 4.2, $Z = 10\text{m/kg}^{1/3}$ and $\eta_c \approx 0.6$. Figure 12(c), for time ratios of 0.08 and 0.3, gives displacement ratios of approximately 0.55 and 1.22. This compares to displacement ratios of 0.54 and 1.23 respectively from the data given in Figure 7.

[2]Providing the assumptions of the Hudson method remain valid, i.e. the shock wave arrives planar and the target has

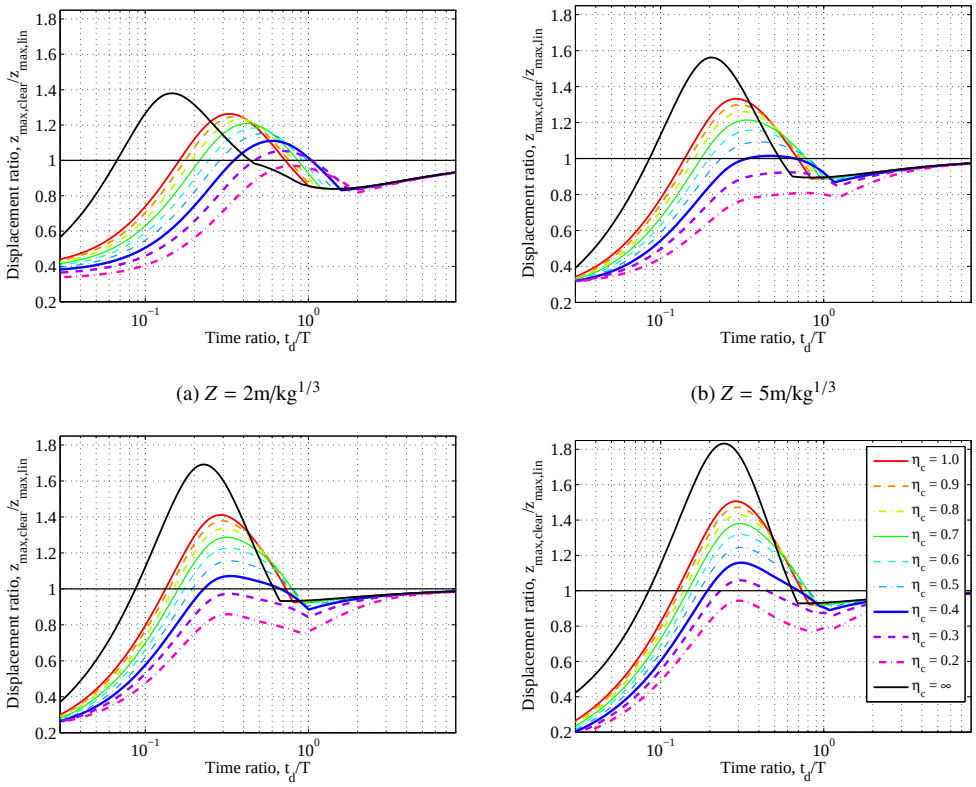

(a) $Z = 2\text{m/kg}^{1/3}$ (b) $Z = 5\text{m/kg}^{1/3}$

(c) $Z = 10\text{m/kg}^{1/3}$ (d) $Z = 20\text{m/kg}^{1/3}$

Figure 12: Response spectra for elastic square targets of varying dimension and dynamic properties, subjected to blast loads at scaled distances of 2, 5, 10 and $20\text{m/kg}^{1/3}$

5. Discussion

The response spectra can be used to make a number of general observations on the scenarios where clearing relief is likely to be a significant factor.

When t_d/T is large, the natural frequency of the system is sufficiently high to ensure that the target reaches its peak displacement before the onset of clearing. For all scaled distances, as the natural period of the structure decreases, the displacement ratio tends towards 1, so it can be said that clearing relief has negligible effect.

When t_d/T is small, the key loading parameter is the net impulse imparted to the target.

sufficient depth, as outlined in section 3.2.

Clearly the consideration of the negative phase alone significantly reduces the total impulse – the displacement ratio for $\eta_c = \infty$ ranges between 0.4–0.6 for the scaled distances studied. The influence of clearing is to reduce the total impulse, further reducing the displacement of the SDOF system. This finding is in agreement with the observations of Ballantyne [21], whereby a series of numerical analyses demonstrated that clearing relief reduces the impulse acting on a finite target by around 50% of the reflected value. In Figure 12, the displacement ratios for finite targets at the impulsive extreme are roughly 0.5 of the displacement ratio for $\eta_c = \infty$. This is particularly true at larger scaled distances.

There exists a region in the dynamic realm of loading, broadly $0.1 < t_d/T < 1.0$, where negative pressures coincide with negative velocities of the target and the result is a greater peak displacement on rebound – an effect which has already been observed for infinite targets [11]. This rebound effect is at its peak when the onset of the negative phase coincides with the peak positive displacement, at the end of the first quarter cycle of displacement, i.e. when $t_d/T = 0.25$. The influence of clearing is to reduce the value of peak displacement, but a reduced positive duration means that this rebound effect occurs at different values of T than would be the case with no clearing. This results in a region where the displacement ratio of the target is *greater* than would be predicted even if negative phase effects were taken into account. In this case, the reduction of pressure initiates 'clearing resonance' and neglecting clearing could be significantly under conservative.

The influence of target size can also be observed – a reduction in target size (η_c) results in more complete clearing relief and, accordingly, reduces the pressure and hence peak displacement of the target. In the clearing resonance region ($0.3 < t_d/T < 1.0$ for $Z = 2\text{m/kg}^{1/3}$), the relationship between target size and displacement ratio is less simple, due to each target size having a different reduced positive phase (see Figure 11). It is acknowledged that clearing resonance requires very specific target properties, however it is important to be aware of the phenomenon and the conditions in which it exists.

These observations are consistent throughout the range of scaled distances studied, with a general trend of increasing displacement ratio with increasing scaled distance. The response spectra can be used to dispel the notion that clearing relief simply acts to reduce the pressure and hence neglecting it is conservative.

It is assumed that the deformed shape of the plate, ϕ, remains constant throughout the anal-

ysis, and that the deformation of the plate and the load are decoupled (i.e. Fluid-Structure Interaction (FSI) effects are not taken into account). Whilst this has been shown to be an important consideration in recent studies [22, 23], it is not the purpose of this article to investigate these effects; it is intended that this study will highlight the implications of neglecting blast wave clearing in a simplistic numerical model. The numerical method outlined in this report may be used in conjunction with other methods pertaining to FSI effects, however, observations made in this article can be used as a first appraisal of the influence of blast wave clearing, and as an indicator as to when a more refined treatment of clearing should be considered.

6. Summary

This paper introduces a simple, accurate, and physically valid means for predicting the spatial and temporal pressure relief associated with blast wave clearing. This method, known as the Hudson method, can be readily combined with the traditional empirical loading model and has shown to demonstrate a remarkable level of accuracy [7].

A spatial load transformation factor, $K_{spatial}$, has been derived as a function of the applied pressure and the normalised deflected shape of the target. This has enabled a spatially non-uniform load to be accurately represented in an SDOF model.

Linear elastic Single-Degree-of-Freedom systems are analysed using a modified load model to take into account the pressure relief caused by clearing, and the values of peak displacement are compared against a traditional SDOF model; a linear system subjected to an equivalent triangular blast load under the assumption that the target is sufficiently large so that edge effects can be neglected. For two sample targets, it is shown that, depending on the dynamic properties of the system, clearing relief may be either beneficial or adverse.

A wider study is conducted by varying both the dimensions of the target (modifying the level of clearing relief) and the dynamic properties (i.e. the fundamental natural period) such that a wide range of target sizes can be considered. The results of which, shown in Figure 12, can be used to quickly determine the effect of clearing on the response of the structure.

For systems where $t_d/T \rightarrow \infty$, clearing has little effect – for systems where $t_d/T \rightarrow 0$, clearing acts favourably; reducing the net impulse and hence the peak displacement of the target.

If the loading lies within the dynamic realm, i.e. the period of the system is similar in magnitude to the duration of the loading event ($0.1 < t_d/T < 1$), negative pressures may coincide with

the ‘rebound’ of the target and result in a greater peak displacement. It is known that clearing may result in early negative pressures, and this effect may initiate ‘clearing resonance’, causing greater peak displacements than would have been predicted had clearing not been considered.

Comprehensive response spectra are presented, taking into account dynamic properties, target sizes and blast scenarios that may be of interest to the engineer. These response spectra enable a first approximation to the influence of clearing relief to be evaluated, giving an indication as to whether clearing is likely to have an impact on the design of the structure. It is observed that a decreasing target size leads to more significant clearing relief, reducing the peak displacement of the target. It is also observed that clearing relief is broadly more significant with larger scaled distances.

When considering far-field events, it is unlikely that key structural members will fail under the prescribed blast pressure, however, lightweight, flexible systems such as cladding and glazing may be particularly prone. The approach outlined in this report offers an effective and powerful means to establish the influence of clearing relief on the dynamic response of finite targets, and can be used as a rapid way to evaluate likely blast damage without relying on computationally expensive methods. Blast wave clearing should be evaluated and its influence quantified in order to ensure blast resistant designs are efficient and safe.

Acknowledgements

The authors would like to express their gratitude to Dr Jim Warren and Mr Roy Mellor of the University of Sheffield Blast & Impact Laboratory and Mr Steve Fay of Blastech Ltd. for designing and conducting the experimental blast trials. The first author acknowledges the financial support from the Engineering and Physical Sciences Research Council (EPSRC) Doctoral Training Grant.

[1] Kingery C, Bulmash G. Airblast parameters from tnt spherical air burst and hemispherical surface burst. Tech. Rep. ARBL-TR-02555; U.S Army BRL, Aberdeen Proving Ground, Maryland, USA; 1984.

[2] Department of Defense. Structures to resist the effects of accidental explosions, United Facilities Criteria (UFC) 3-340-02; 2008.

[3] Hyde D. Conventional Weapons Program (ConWep). U.S Army Waterways Experimental Station, Vicksburg, USA; 1991.

[4] U.S. Army Corps of Engineers. Methodology manual for the Single-Degree-of-Freedom Blast Effects Design Spreadsheets (SBEDS), PDC TR-06-01; 2008.

[5] Rickman DD, Murrell DW. Development of an improved methodology for predicting airblast pressure relief on a directly loaded wall. Journal of Pressure Vessel Technology 2007;129(1):195–204.

[6] Rose T, Smith P. An approach to the problem of blast wave clearing on finite structures using empirical procedures based on numerical calculations. In: 16th Symposium on the Military Aspects of Blast and Shock (MABS16). Oxford, UK; 2000, p. 113–20.

[7] Tyas A, Warren J, Bennett T, Fay S. Prediction of clearing effects in far-field blast loading of finite targets. Shock Waves 2011;21:111–9.

[8] Tyas A, Bennett T, Warren J, Fay S, Rigby SE. Clearing of blast waves on finite-sized targets, an overlooked approach. Applied Mechanics and Materials 2011;82:669–74.

[9] Hudson C. Sound pulse approximations to blast loading (with comments on transient drag). Tech. Rep. SC-TM-191-55-51; Sandia Corporation, Maryland, USA; 1955.

[10] Baker WE. Explosions in air. University of Texas Press, Austin; 1973.

[11] Teich M, Gebbeken N. The influence of the underpressure phase on the dynamic response of structures subjected to blast loads. International Journal of Protective Structures 2010;1:219–34.

[12] Krauthammer T, Altenberg A. Negative phase blast effects on glass panels. International Journal of Impact Engineering 2000;24(1):1 – 17.

[13] Goodman H. Compiled free-air blast data on bare spherical pentolite. Tech. Rep. ARBL-TR-1092; U.S Army BRL, Aberdeen Proving Ground, Maryland, USA; 1960.

[14] Naval Facilities Engineering Command (NavFac). Blast resistant structures, NFE DM 2-08; 1986.

[15] Bogosian D, Ferritto J, Shi Y. Measuring uncertainty and conservatism in simplified blast models. In: 30th Explosives Safety Seminar. Atlanta, Georgia, USA; 2002, p. 1–26.

[16] Biggs J. Introduction to structural dynamics. McGraw-Hill, New York; 1964.

[17] Blevins RD. Formulas for natural frequency and mode shape. Van Nostrand Reinhold Co., New York; 1979.

[18] Morison CM. Dynamic response of walls and slabs by single-degree-of-freedom analysis–a critical review and revision. International Journal of Impact Engineering 2006;32(8):1214 –47.

[19] Hallquist JO. LS-DYNA Theory Manual. Livermore Software Technology Corporation, California; 2006.

[20] Shi Y, Hao H, Li ZX. Numerical simulation of blast wave interaction with structure columns. Shock Waves 2007;17:113–33.

[21] Ballantyne GJ, Whittaker AS, Dargush GF, Aref AJ. Air-blast effects on structural shapes of finite width. Journal of Structural Engineering 2010;136(2):152 –9.

[22] Kambouchev N, Noels L, Radovitzky R. Numerical simulation of the fluid-structure interaction between air blast waves and free-standing plates. Computers & Structures 2007;85(11 - 14):923 –31.

[23] Subramaniam KV, Nian W, Andreopoulos Y. Blast response simulation of an elastic structure: Evaluation of the fluid-structure interaction effect. International Journal of Impact Engineering 2009;36(7):965 –74.